

## Structural Studies of the Resistance of Influenza Virus Neuraminidase to Inhibitors

Brian J. Smith,<sup>\*,†</sup> Jennifer L. McKimm-Breshkin,<sup>‡</sup> Mandy McDonald,<sup>‡</sup> Ross T. Fernley,<sup>‡</sup> Joseph N. Varghese,<sup>‡</sup> and Peter M. Colman<sup>†</sup>

*The Walter and Eliza Hall Institute of Medical Research, P.O. Royal Melbourne Hospital, Parkville, Victoria 3050, Australia, and Division of Health Sciences and Nutrition, CSIRO, Parkville, Victoria 3052, Australia*

Received November 19, 2001

Zanamivir and oseltamivir, specific inhibitors of influenza virus neuraminidase, have significantly different characteristics in resistance studies. In both cases resistance is known to arise through mutations in either the hemagglutinin or neuraminidase surface proteins. A new inhibitor under development by Biocryst Pharmaceuticals, BCX-1812, has both a guanidino group, as in zanamivir, and a bulky hydrophobic group, as in oseltamivir. Using influenza A/NWS/Tern/Australia/G70C/75 (H1N9), neuraminidase variants E119G and R292K have previously been selected by different inhibitors. The sensitivity of these variants to BCX-1812 has now been measured and found in both cases to be intermediate between those of zanamivir and oseltamivir. In addition, the X-ray crystal structures of the complexes of BCX-1812 with the wild type and the two mutant neuraminidases were determined. The ligand is bound in an identical manner in each structure, with a rearrangement of the side chain of E276 from its ligand-free position. A structural explanation of the mechanism of resistance of BCX-1812, relative to zanamivir and oseltamivir in particular, is provided.

### Introduction

Vaccines against influenza virus are often ineffective due to the rapid emergence of mutant viral antigens. The compounds amantadine and rimantadine, which block the M2 protein ion channel function, are effective only against type A influenza and produce undesirable side effects, and resistant mutants are rapidly generated. Antiviral treatment for influenza virus infection now also includes the neuraminidase (NA) inhibitors zanamivir and oseltamivir. Resistance *in vitro* to these anti-infective agents is due to mutations in the hemagglutinin and neuraminidase proteins.<sup>1</sup> Resistance *in vivo* has so far only been mapped to mutations in the NA.

The development of zanamivir, oseltamivir, and BCX-1812 have all been based on the knowledge of the structure of the NA with its natural substrate sialic acid.<sup>2</sup> While zanamivir and oseltamivir are now both registered internationally, BCX-1812 is still in phase 3 trials.<sup>3</sup> As part of an evaluation of the development of resistance to NA inhibitors we have previously generated two NWS/G70C (H1N9) influenza viruses with mutations in their NAs R292K<sup>4</sup> and E119G,<sup>5</sup> which have different resistance profiles to zanamivir and oseltamivir. We have used structural information to provide an understanding of the mechanism of resistance of these NA mutants to a panel of NA inhibitors including zanamivir and oseltamivir.<sup>5,6</sup>

BCX-1812 maintains many structural similarities with both zanamivir and oseltamivir (Figure 1). All contain a carboxylate group (oseltamivir is the ethyl ester of the active form of the compound that is activated

by hepatic esterases) that binds the triad of arginyl side chains R118, R292, and R371, and an *N*-acetyl group that binds the small hydrophobic pocket formed predominantly by the side chains I222 and W178. While the cyclopentane core of BCX-1812 distinguishes it from zanamivir and oseltamivir, it contains features that relate it to both: the guanidinium group at the 4 position of zanamivir, and the bulky hydrophobic group at the 6 position like that in oseltamivir.<sup>7</sup>

We have previously advocated a minimalist approach to drug design; the closer the inhibitor is to the natural substrate the less likelihood that the target can mutate without loss of the natural function.<sup>6</sup> As BCX-1812 has modifications at residues corresponding to both the 4 and 6 positions (in sialic acid), this presents two potential targets for mutation. BCX-1812 has been reported to be less resistant than zanamivir to the E119G mutant,<sup>7,8</sup> and less resistant than oseltamivir to the R292K mutant,<sup>9</sup> in an N2 variant of NA. We compare here the relative sensitivity of the NWS/G70C (H1N9) R292K and E119G NA mutants to BCX-1812 in an enzyme inhibition assay and have used X-ray crystallography to help clarify the mechanisms of resistance.

### Results

**Enzyme Inhibition Data.** As shown in Table 1 both mutants demonstrated some resistance to BCX-1812, but the magnitudes of resistance were different from those seen with zanamivir and oseltamivir. The R292K mutant was 1000-fold less sensitive to BCX-1812 than the wild-type enzyme. This was significantly higher than the resistance of this mutant to zanamivir, but lower than the resistance to oseltamivir. The E119G was 50-fold less sensitive to BCX-1812, which was less than

\* To whom correspondence should be addressed. Phone: +61 (3) 9662 7289. Fax: +61 (3) 9662 7347. E-mail: bsmith@wehi.edu.au.

<sup>†</sup> The Walter and Eliza Hall Institute of Medical Research.

<sup>‡</sup> CSIRO.

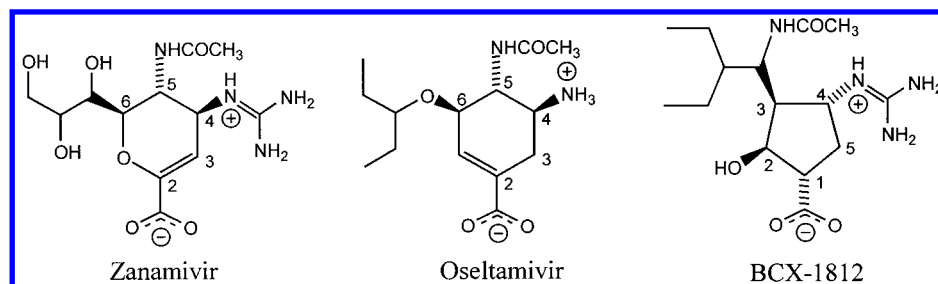


**Figure 1.** Structures of the neuraminidase inhibitors zanamivir, oseltamivir (active form), and BCX-1812.

**Table 1.** Fold Resistance of E119G and R292K to NA Inhibitors in a MUNANA-Based Enzyme Inhibition Assay<sup>a</sup>

neuraminidase	BCX-1812	zanamivir <sup>b</sup>	oseltamivir <sup>b,c</sup>	carboxamide <sup>d</sup>
E119G	50	250	1	nd
R292K	1000	55	6500	795

<sup>a</sup> Fold resistance refers to the ratios of the IC<sub>50</sub> of the compound with the variant N9 to the IC<sub>50</sub> of the compound with wild-type N9. <sup>b</sup> Reference 1. <sup>c</sup> Resistance is to the activated form of the prodrug. <sup>d</sup> Reference 4. Methylpropyl-6-carboxamide of Neu5Ac2en.

the resistance of this mutant to zanamivir, but greater than the resistance to oseltamivir.

**Structure of the BCX-1812:Wild-Type N9 Complex.** The inhibitor appeared as a large positive feature in the difference Fourier maps, clearly showing the position of all component atoms. The structure of the complex of BCX-1812 and wild-type N9 NA determined here is identical in all features to that reported previously<sup>7</sup> (Figure 2a). The functional groups common between BCX-1812 and zanamivir, the carboxylate, *N*-acetyl, and guanidinium groups, all have the same relative positions in the active site. The carboxylate forms salt bridges with the guanidinium groups of R118, R371, and R292. The carbonyl oxygen of the *N*-acetyl group forms a hydrogen bond with a distal nitrogen atom of the side chain of R151, while the amide nitrogen forms a hydrogen bond with a water molecule at the base of the active site. The guanidinium group interacts with the acidic groups E119 and E227.

Examination of positive and negative features in the  $F_o - F_c$  difference maps about E276 indicated an altered side chain configuration from the ligand-free structure. Difference Fourier maps in which E276 had been removed revealed a reorientation of its side chain. This reorganization of the active site presents a hydrophobic pocket into which the 2'-ethyl group binds. In the ligand-free structure one of the carboxylate oxygen atoms of E276 forms a single salt bridge with the distal nitrogen atom of the guanidinium group of R224. In the rearrangement of the side chain of E276 both carboxylate oxygen atoms form salt bridges, to the N<sub>ε</sub> and a distal nitrogen atom of R224. The same rearrangement is seen in the NA complexes with oseltamivir, the 6-carboxamides of Neu5Ac2en,<sup>6</sup> pyrrolidine-based inhibitors,<sup>13</sup> and certain benzoic acid inhibitors.<sup>14</sup>

**Structure of the R292K Variant:BCX-1812 Complex.** The location of the ligand could be clearly resolved from the difference Fourier electron density maps. The mutation at 292 was confirmed by the presence of a feature consistent with a lysine side chain, previously occupied by arginine in the wild-type structure. The conformation of the side chain at E276 could be clearly resolved to be the same as that found in the wild-type structure with inhibitor bound.

R292 is one of the triad of arginines in the active site that engages the substrate carboxylate. These arginines are thought to be partly responsible for distortion of the pyranose ring of the substrate from the low-energy chair conformation to the twist-boat conformation. In the ligand-free mutant structure<sup>6</sup> the amino group of the K292 forms an ionic interaction with E276, and water molecules replace the missing distal nitrogen atoms of the guanidinium group of R292.

In the structure of the complex of the R292K mutant with BCX-1812 the ligand occupies the same position in the active site as that found in the wild-type NA (Figure 2b). The K292 N<sub>ε</sub> nitrogen forms an ionic interaction with one of the carboxylate oxygen atoms of E277 (2.79 Å). In the ligand-free mutant this interaction is significantly weaker (3.28 Å). Thus, the structure of the BCX-1812 NA complex differs from that of the zanamivir and oseltamivir complexes with the R292K variant predominantly by a small (roughly 0.5 Å) displacement of the side chains of E277 and K292. A similar change is also observed for the diethyl-6-carboxamide of Neu5Ac2en.<sup>6</sup> The water molecule that replaces one of the distal guanidinium nitrogen atoms of the arginine side chain connecting K292 with E277 and Y406 is not observed in either the BCX-1812:R292K mutant or diethyl-6-carboxamide:R292K mutant complex, presumably because it is unable to be accommodated within the restricted space formed by the closer association of the side chains of E277 and K292.

**Structure of the E119G Variant:BCX-1812 Complex.** Examination of the difference maps revealed no side chain density corresponding to E119, consistent with the E119G mutation. Again, the location of the inhibitor could be clearly resolved, and the conformation of the side chain at E276 was the same as that found for the inhibitor-bound wild-type and R292K mutant structures.

The carboxylate side chain of E119 is replaced by a water molecule in the E119G mutant. The position in the active site of this water molecule is the same as that observed previously for the complex with zanamivir.<sup>5</sup> The ligand binds identically in this mutant, the wild type, and the R292K mutant complexes (Figure 2c).

The C5 atom of BCX-1812 makes the closest approach to the carboxylate oxygen atoms of E119, 3.25 Å. In comparison, the distance between the carboxylate oxygen and C3 atom in zanamivir is 3.58 Å.<sup>15</sup> We have attempted to obtain some indication of the relative interaction energies of the methyl and methylene moieties in these two systems through molecular orbital calculations on small model systems.

The relative dissociation energies of the complexes of propane and propene with acetic acid (Figure 3) provide



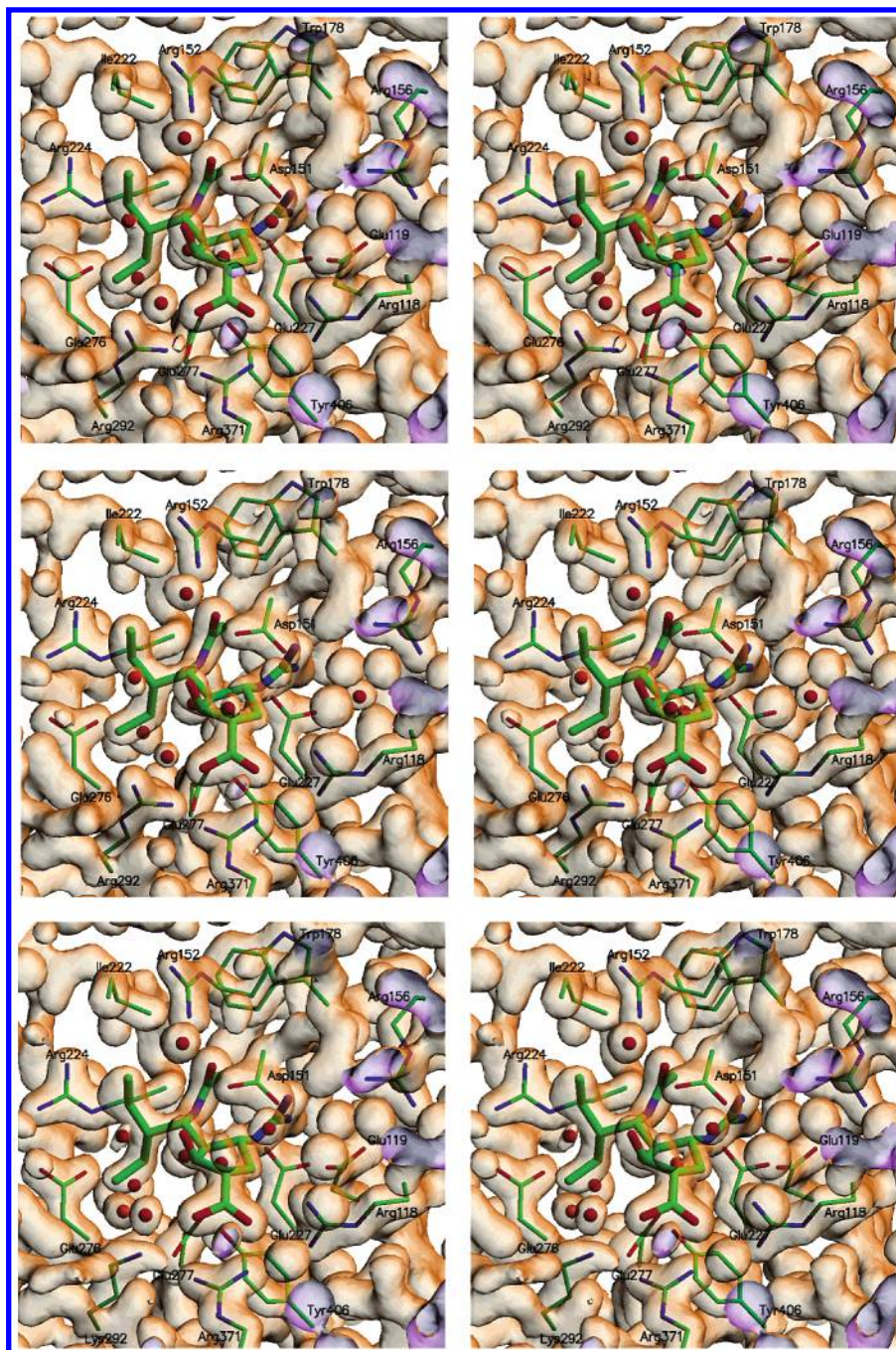


**Figure 2.** Stereo diagram of BCX-1812 bound in the active site of neuraminidase: (a) wild-type enzyme, (b) E119G mutant, and (c) R292K mutant. Only amino acid side chains of active site residues are shown; spheres are water molecules. Residues are overlaid with an electron density isosurface generated at the  $1.5\sigma$  level from the  $2F_o - F_c$  electron density of the refined model. This diagram was generated using CONSCRIPT,<sup>10</sup> MOLSCRIPT,<sup>11</sup> and Raster3D.<sup>12</sup>

a qualitative estimate of the relative interaction energies. The interaction of propene with acetic acid is  $8.7 \text{ kJ mol}^{-1}$  larger than the interaction of propane with acetic acid, despite the larger separation between the acetic acid carboxylate oxygen atom and the  $\text{sp}^2$  carbon of propene compared with that of the  $\text{sp}^3$  carbon of propane.

## Discussion

In contrast to oseltamivir, both NWS/G70C mutants were resistant to BCX-1812 in an enzyme inhibition assay. However, resistance to BCX-1812 was less for the R292K mutant than that to oseltamivir. The resistance of the R292K mutant to BCX-1812 was comparable to

the resistance to the methylpropyl-6-carboxamide analogue of zanamivir.<sup>4</sup> The E119G mutant was not as resistant to BCX-1812 as to zanamivir.

Zanamivir and oseltamivir have different resistance profiles, due to the modification of different groups on the core structure. The carboxylate of the E119 side chain interacts with the 4-guanidino group on zanamivir, and loss of this interaction in the E119G mutant leads to a decrease in binding of zanamivir. There is also an additional water molecule in the position previously occupied by the carboxylate side chain. Hence, altered binding of zanamivir is through both loss of interaction of the carboxylate side chain with the guanidinium group and alterations in the solvent struc-

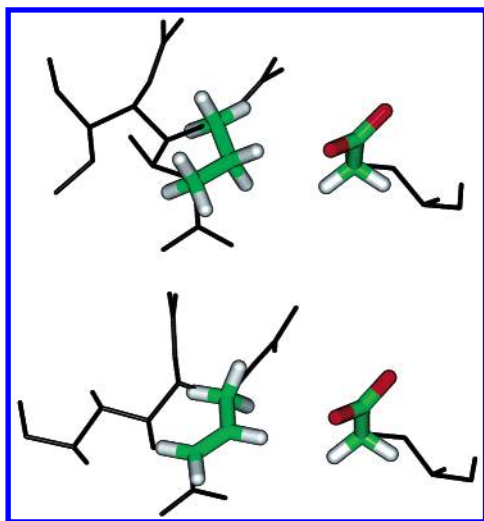


**Figure 3.** Structures of complexes of propane and propene with acetic acid overlaid on the X-ray structures of BCX-1812 and zanamivir bound to the active site of neuraminidase.

ture.<sup>5</sup> Oseltamivir has an ammonium group at the 4 position, and does not form the close association with E119 as does the guanidinium group of zanamivir. It is unaffected by the E119G mutation. Since BCX-1812 has a guanidinium group (like zanamivir), one might expect the E119G mutant would also demonstrate resistance to BCX-1812. However, resistance was not as great as to zanamivir in an enzyme inhibition assay. Structural analysis of the E119G:BCX-1812 complex revealed that the guanidino groups of the two ligands are almost coplanar, and that the additional water molecule (which replaces the E119 carboxylate side chain of the wild-type enzyme) occupies a position almost identical to that found in the zanamivir complex.

Molecular orbital calculations show that the interaction of acetic acid with propene is greater than the interaction with propane. The difference of the interaction energies is roughly a factor of 2 larger than that required to account for the difference in sensitivity between zanamivir and BCX-1812. The molecular orbital calculations indicate that zanamivir has a stronger interaction with E119 than BCX-1812 due to the formation of a weak ionic hydrogen bond. This may account for the increased resistance of the E119G mutant to zanamivir.

The R292K mutation affects binding of the bulky hydrophobic side chain in oseltamivir by several orders of magnitude, but has only a small effect on binding of zanamivir. Binding of oseltamivir requires reorientation of E276 to form a salt link to R224, to accommodate the bulky hydrophobic side chain at the 6 position. In the case of the R292K variant the salt link between K292 and E276 must be broken to allow the reorientation of E276.<sup>6</sup> However, the energy penalty is too great to permit the creation of the binding pocket for the pentyl ether of oseltamivir, resulting in 10000-fold resistance to oseltamivir in an enzyme assay.<sup>4,16</sup> In the case of the methylpropyl-6-carboxamide analogue of zanamivir binding is also significantly reduced, by approximately 1000-fold, but the reorientation to accommodate the carboxamide side chain does occur.<sup>4</sup>

Determination of the structure of the R292K NA:BCX-1812 complex revealed a similarity to the binding of the

methylpropyl-6-carboxamide analogue of zanamivir.<sup>6</sup> In both cases reorientation of E276 occurs. The magnitude of resistance in an enzyme assay for these two compounds was similar. An overlay of the structures reveals the carboxylate, *N*-acetyl, and guanidinium groups occupy very similar positions. The 6-carboxamide and 2'-propyl groups, however, occupy quite different positions in the hydrophobic pocket generated by the reorientation of E276.

Reorganization of E276 to form the hydrophobic pocket thus appears to be a prerequisite for tight binding of inhibitors with a hydrophobic side chain. Since oseltamivir fails to induce the conformational change of E276 in the R292K mutant NA, it is unable to engage the active site as it does in the wild-type NA, and consequently it binds less tightly than to the wild-type NA. We have attempted to predict how oseltamivir might bind if reorientation of E276 were to occur, by performing a superimposition of the protein backbone atoms of the R292K NA mutants from the complexes with either the methylpropyl-6-carboxamide or BCX-1812 inhibitor, with the protein backbone atoms of the complex of oseltamivir with wild-type NA. In the former of these two comparisons a very short contact (2.94 Å) would be made between one of the terminal methyl groups of the diethyl side chain of oseltamivir with the N<sub>ε</sub> ammonium nitrogen of K292. However, this short contact is relieved (3.64 Å) when oseltamivir is placed into the R292K mutant NA obtained from the BCX-1812 complex. In this latter comparison, no unusually short nonbonded contacts are predicted. Thus, oseltamivir should be able to engage the active site with the reorganization of E276.

Oseltamivir binds in a different conformation in native and R292K N9; the torsional angle about the ether bond (C6–O) differs by more than 40°. Qualitatively, oseltamivir is the least conformationally restricted of all the ligands to the structures observed in complex with wild-type neuraminidase. Although other factors must play a role, this observation is not inconsistent with oseltamivir's failure to induce the conformational change in E276.

A very different profile of resistance has been observed for these compounds in N2 variants of neuraminidase.<sup>8,9</sup> The R292K mutant in the A/Singapore 1/57 virus is only 10–20-fold resistant to both zanamivir and BCX-1812, while oseltamivir is 5000-fold resistant.<sup>9</sup> Similar resistance to BCX-1812 has been reported in N2 from turkey with this mutation, whereas it causes 10000-fold resistance to oseltamivir. The E119G variant of turkey N2 is as sensitive to BCX-1812 as wild-type NA.<sup>8</sup> Thus, BCX-1812 displays lower resistance to both E119G and R292K mutants in the N2 background compared to the N9. BCX-1812 distinguishes the subtle differences between the active site structures of N2 and N9 NA to a greater degree than does either zanamivir or oseltamivir.

We have proposed that the energy required for reorientation of the side chain of E276 is the origin of the resistance of the R292K variant toward compounds such as BCX-1812 with a large hydrophobic group.<sup>6</sup> The large difference in sensitivity of the N2 and N9 R292K mutants toward BCX-1812 suggests a reduced energy requirement for the reorganization of the active site in



the N2 variant compared to N9. The reorganization of E276 in the NA from influenza B has been shown from molecular dynamics simulations to occur less frequently than in NA from influenza A.<sup>17</sup> The difference in the energy penalty accounts for the selectivity of inhibitors that require this reorientation for binding. However, in both N2 and N9 backgrounds the R292K variant shows similarly high resistance to oseltamivir. The energy penalty for the conformational change in E276 is presumably not the only determinant of the resistance of R292K to oseltamivir.

## Materials and Methods

**Viruses.** The wild-type reassortant influenza virus A/NWS/Tern/Australia/G70C/75 was originally obtained from Dr. R. Webster (Memphis, TN). Variants with the R292K and E119G mutations were generated after passaging this virus in the presence of zanamivir<sup>5</sup> and the methylpropyl-6-carboxamide analogue of zanamivir<sup>4</sup> as previously described.

**Enzyme Inhibition Assays.** Wild-type and mutant viruses were tested for sensitivity to BCX-1812 in an enzyme inhibition assay using methyl umbelliferone *N*-acetyl neuraminic acid (MUNANA) as the substrate, as previously described.<sup>5</sup> Briefly, viruses or purified NAs were titrated to determine a dilution that gave a value in the linear range of the activity curve. This dilution was then incubated with serial 2-fold dilutions of the inhibitor for 30 min, prior to the addition of substrate. The reaction was stopped after 1 h by the addition of sodium carbonate. Fluorescence was read on a Perkin-Elmer fluorimeter using an excitation wavelength of 365 nm and an emission wavelength of 450 nm.

**X-ray Crystal Structure Analysis.** The NA was purified as previously described.<sup>18</sup> Crystals of G70C wild-type and mutant NAs were grown by established procedures<sup>19</sup> in 1.9 M phosphate (pH 5.9). Crystals were soaked in buffered solution containing 2–3 mM inhibitor for 1 h, transferred to 20% glycerol solution, and flash frozen to 100 K in a stream of cold nitrogen (Oxford Instruments, Oxford, England). X-ray data for the wild-type and R292K mutant crystals were collected on an *R*-axis IV IP detector, using a Rigaku generator operating at 40 kV and 20 mA, and fitted with elliptical glass monocapillary optics using a 0.1 mm focus at the crystal.<sup>20</sup> The E119G mutant data were collected on an *R*-axis IV IP detector mounted on a MAC-Science SRAM 18XH1 rotating anode X-ray generator, operating at 40 kV and 50 mA with focusing mirrors. All diffraction data were collected using 0.5° oscillations and 1 h exposure times, and were analyzed with *hkl*.<sup>21</sup> The space group is *I*432. Statistics of individual data sets are given in Table 2.

The location of the ligand bound to the wild-type and two mutant NAs was determined with difference Fourier methods using phases from the ligand-free structures.<sup>6</sup> All solvent molecules, and side chain atoms at residues 292 and 119 in the R292K and E119G mutants, respectively, were initially removed. Manual rebuilding and repositioning of atoms in the model structures was performed using "O".<sup>22</sup> Waters were added automatically to statistically significant density using *WARP*.<sup>23</sup> Final refinement was conducted using *REFMAC*<sup>24</sup> and included a bulk solvent correction and restrained *B*-factor refinement. The quality of the final models was checked using *PROCHECK*.<sup>25</sup> The atomic coordinates and structure factors have been deposited with the Protein Data Bank with the following accession codes: wild type, 1L7F; R292K, 1L7H; E119G, 1L7G.

**Quantum Mechanics.** Standard ab initio molecular orbital calculations<sup>26</sup> were performed using the GAMESS-US package.<sup>27</sup> Geometries were optimized at the MP2(full)/6-31G(d) level with flat-bottomed harmonic restraints. Heavy atoms were restrained to their X-ray structure positions with a force constant of 5.0 aJ Å<sup>-2</sup> and a switch distance of 0.1 Å. These restraints allow the system to relax from the experimental geometry without allowing large changes in the positions of

**Table 2.** Data Collection and Crystallographic Refinement Statistics

	wild type	R292K	E119G
Data Collection			
unit cell <i>a</i> (Å)	181.12	180.83	180.75
resolution range (Å)	20.0–1.80	20.0–1.85	20.0–1.85
no. of total observations	453337	337369	347312
no. of unique observations	46825	42540	43185
<i>R</i> <sub>merge</sub> <sup>a,b</sup>	0.15 (0.58)	0.08 (0.38)	0.08 (0.76)
$\langle I/\sigma(I) \rangle^a$	28.5 (3.2)	23.3 (2.4)	26.3 (2.6)
data completeness (%) <sup>a</sup>	100.0 (100.0)	98.6 (89.3)	100.0 (100.0)
Refinement			
resolution Range (Å)	6.0–1.80	6.0–1.85	6.0–1.85
no. of reflections			
working set	43167	39007	39450
free set	2289	2060	2092
<i>R</i> <sub>cryst</sub>	0.153	0.145	0.148
<i>R</i> <sub>free</sub>	0.187	0.177	0.168
no. of atoms/monomeric unit			
protein <sup>c</sup>	3210	3213	3210
solvent	662	588	593
ligand	23	23	23
rms dev from ideality (Å)			
bond distance	0.008	0.008	0.008
angle distance	0.025	0.026	0.026
planar 1–4 distance	0.023	0.022	0.024
av <i>B</i> -factors (Å <sup>2</sup> )			
main chain	18.2	18.8	23.1
side chain	19.9	20.3	24.5
solvent	37.6	37.0	40.8
ligand	18.0	18.2	22.5

<sup>a</sup> Numbers in parentheses refer to the statistic in the outer shell.

<sup>b</sup>  $R_{\text{merge}} = \sum hkl (\sum i |I_{hkl,i} - \langle I_{hkl} \rangle|) / \sum hkl \sum i I_{hkl,i}$ . <sup>c</sup> Includes carbohydrate.

loosely associated groups. Calculations were performed on complexes of propane with the acetate anion and of propene with acetate. Atoms in the acetate group were restrained to the X-ray positions of the side chain of E119, while the atoms of propene and propane were restrained to the X-ray positions of the C2, C3, and C4 atoms of zanamivir and BCX-1812, respectively. Energies are reported at the MP2(fc)/6-311+G-(2df,p) level. Basis set superposition errors (BSSEs) are evaluated using the counterpoise correction method. All energies reported have BSSE corrections applied.

**Acknowledgment.** We are very grateful to Bert van Donkelaar and Pat Pilling for technical assistance. BCX-1812 was provided by GlaxoSmithKline Research and Development (Stevenage, U.K.).

## References

- McKimm-Breshkin, J. L. Resistance of influenza viruses to neuraminidase inhibitors—a review. *Antiviral Res.* **2000**, *47*, 1–17.
- Varghese, J. N.; McKimm-Breshkin, J. L.; Caldwell, J. B.; Kortt, A. A.; Colman, P. M. The structure of the complex between influenza virus neuraminidase and sialic acid, the viral receptor. *Proteins* **1992**, *14*, 327–332.
- Barnard, D. L. RWJ-270201 BioCryst pharmaceuticals/Johnson & Johnson. *Curr. Opin. Invest. Drugs* **2000**, *1*, 421–424.
- McKimm-Breshkin, J. L.; Sahasrabudhe, A.; Blick, T. J.; McDonald, M.; Colman, P. M.; Hart, G. J.; Bethell, R. C.; Varghese, J. N. Mutations in a conserved residue in the influenza virus neuraminidase active site decreases sensitivity to Neu-5-Ac2en-derived inhibitors. *J. Virol.* **1998**, *72*, 2456–2462.
- Blick, T. J.; Tiong, T.; Sahasrabudhe, A.; Varghese, J. N.; Colman, P. M.; Hart, G. J.; Bethell, R. C.; McKimm-Breshkin, J. L. Generation and characterisation of an influenza virus neuraminidase variant with decreased sensitivity to the neuraminidase-specific inhibitor 4-guanidino-Neu5Ac2en. *Virology* **1995**, *214*, 475–484.
- Varghese, J. N.; Smith, P. W.; Sollis, S. L.; Blick, T. J.; Sahasrabudhe, A.; McKimm-Breshkin, J. L.; Colman, P. M. Drug design against a shifting target: a structural basis for resistance to inhibitors in a variant of influenza virus neuraminidase. *Structure* **1998**, *6*, 735–746.

- (7) Babu, Y. S.; Chand, P.; Bantia, S.; Kotian, P.; Dehghani, A.; El-Kattan, Y.; Lin, T.; Hutchison, T. L.; Elliot, A. J.; Parker, C. D.; Ananth, S. L.; Horn, L. L.; Laver, G. W.; Montgomery, J. A. BCX-1812 (RWJ-270201): Discovery of a novel, highly potent, orally active, and selective influenza neuraminidase inhibitor through structure-based drug design. *J. Med. Chem.* **2000**, *43*, 3482–3486.
- (8) Gubareva, L.; Webster, R. G.; Hayden, F. G. Cross-resistance of influenza mutants to NA inhibitors: zanamivir, GS4071 and RWJ-270201. *Antiviral Res.* **2000**, *46*, A54.
- (9) Bantia, S.; Anath, S.; Horn, L.; Parker, C.; Gulati, U.; Chand, P.; Babu, Y.; Air, G. Generation and characterization of a mutant of influenza A virus selected with neuraminidase inhibitor RWJ-270201. *Antiviral Res.* **2000**, *46*, A60.
- (10) Lawrence, M. C.; Burke, P. CONSCRIPT: a program for generating electron density isosurfaces for presentation in protein crystallography. *J. Appl. Crystallogr.* **2000**, *33*, 990–991.
- (11) Kraulis, P. J. MOLSCRIPT: A program to produce both detailed and schematic plots of protein structures. *Appl. Crystallogr.* **1991**, *24*, 946–950.
- (12) Merrit, E. A.; Bacon, D. J. Raster3D: Photorealistic molecular graphics. *Methods Enzymol.* **1997**, *277*, 505–524.
- (13) Wang, G. T.; Chen, Y.; Wang, S.; Gentles, R.; Sowin, T.; Kati, W.; Muchmore, S.; Giranda, V.; Stewart, K.; Sham, H.; Kempf, D.; Laver, W. G. Design, synthesis, and structural analysis of influenza neuraminidase inhibitors containing pyrrolidine cores. *J. Med. Chem.* **2001**, *44*, 1192–1201.
- (14) Atigadda, V. R.; Brouillette, W. J.; Duarte, F.; Ali, S. M.; Babu, Y. S.; Bantia, S.; Chand, P.; Chu, N.; Montgomery, J. A.; Walsh, D. A.; Sudbeck, E. A.; Finley, J.; Luo, M.; Air, G. M.; Laver, G. W. Potent inhibition of influenza sialidase by a benzoic acid containing a 2-pyrrolidinone substituent. *J. Med. Chem.* **1999**, *42*, 2332–2343.
- (15) Varghese, J. N.; Epa, V. C.; Colman, P. M. Three-dimensional structure of the complex of 4-guanidino-Neu5Ac2en and influenza virus neuraminidase. *Protein Sci.* **1995**, *4*, 1081–1087.
- (16) Tai, C. Y.; Escarpe, P. A.; Sidwell, R. W.; Williams, M. A.; Lew, W.; Wu, H. W.; Kim, C. U.; Mendel, B. B. Characterization of human influenza virus variants selected in vitro in the presence of the neuraminidase inhibitor GS 4071. *Antimicrob. Agents Chemother.* **1998**, *42*, 3234–3241.
- (17) Taylor, N. R.; Cleasby, A.; Singh, O.; Skarzynski, T.; Wonacot, A. J.; Smith, P. W.; Sollis, S. L.; Howes, P. D.; Cherry, P. C.; Bethell, R.; Colman, P. M.; Varghese, J. Dihydropyranocarboxamides related to zanamivir: A new series of inhibitors of influenza virus sialidases. 2. Crystallographic and molecular modeling study complexes of 4-amino-4H-pyran-6-carboxamides and sialidase from influenza virus types A and B. *J. Med. Chem.* **1998**, *41*, 798–807.
- (18) McKimm-Breshkin, J. L.; Caldwell, J. B.; Guthrie, R. E.; Kortt, A. A. A new method for the purification of influenza A virus. *J. Virol. Methods* **1991**, *32*, 121–124.
- (19) Laver, W. G.; Colman, P. M.; Webster, R. G.; Hinshaw, V. S.; Air, G. M. Influenza virus neuraminidase with hemagglutinin activity. *Virology* **1984**, *137*, 314–323.
- (20) Baliac, D. X.; Barnea, Z.; Nugent, K. A.; Garrett, R. F.; Varghese, J. N.; Wilkins, S. W. Protein crystal diffraction patterns using a capillary-focused X-ray beam. *J. Synchrotron Radiat.* **1996**, *3*, 289–295. Varghese, J. N.; van Donkelaar, A.; Hrmova, M.; Fincher, G. B.; Baliac, D. X.; Barnea, Z. A structure of exoglucanase complexed with conduritol B epoxide from 30  $\mu\text{m}^3$  crystal using monocapillary optics, VXIIIth IUCR Congress, 1999, *Acta Cryst.* A55 Suppl.
- (21) Otwinowski, Z.; Minor, W. A processing of X-ray diffraction data collection in oscillation mode. *Methods Enzymol.* **1996**, *276*, 307–326.
- (22) Jones, T. A.; Zou, J. Y.; Cowan, S. W.; Kjeldgaard, M. Improved methods for building protein models in electron density maps and the location of errors in these models. *Acta Crystallogr.* **1991**, *A47*, 110–119.
- (23) Perrakis, A.; Sixma, T. K.; Wilson, K. S.; Lamzin, V. S. wARP: Improvement and extension of crystallographic phases by weighted averaging of multiple refined dummy atomic models. *Acta Crystallogr.* **1997**, *D53*, 448–455.
- (24) Murshudov, G. N.; Vagin, A. A.; Dodson, E. J. Refinement of macromolecular structures by the maximum-likelihood method. *Acta Crystallogr.* **1997**, *D53*, 240–255.
- (25) Laskowski, R. A.; MacArthur, M. W.; Moss, D. S.; Thornton, J. M. PROCHECK: a program to check the stereochemical quality of protein structures. *J. Appl. Crystallogr.* **1993**, *26*, 283–291.
- (26) Hehre, W. J.; Radom, L.; Schleyer, P. v. R.; Pople, J. A. *Ab Initio Molecular Orbital Theory*; Wiley-Interscience: New York, 1986.
- (27) Schmidt, M. W.; Baldrige, K. K.; Boatz, J. A.; Elbert, S. T.; Gordon, M. S.; Jensen, J. H.; Koseki, S.; Matsunaga, N.; Nguyen, K. A.; Su, S. J.; Windus, T. L.; Dupuis, M.; Montgomery, J. A. General atomic and molecular electronic structure system. *J. Comput. Chem.* **1993**, *14*, 1347–1363.

JM010528U